Organic & Biomolecular Chemistry

Dynamic Article Links

Cite this: *Org. Biomol. Chem.*, 2012, **10**, 791

www.rsc.org/obc

PAPER

C^{α}–C^{β} and C^{α}–N bond cleavage in the dissociation of protonated *N*–benzyllactams: dissociative proton transfer and intramolecular proton-transport catalysis†

Yunfeng Chai, Cheng Guo, Kezhi Jiang, Yuanjiang Pan* and Cuirong Sun*

Received 25th June 2011, Accepted 14th October 2011
DOI: 10.1039/c1ob06020a

In mass spectrometry of protonated *N*-benzylbutyrolactams, the added proton is initially localized on the carbonyl oxygen, which is the thermodynamically preferred protonation site. Upon collisional activation, dissociative proton transfer takes place leading to the occurrence of fragmentation reactions. The major fragmentations observed are the cleavages of C^{α}–C^{β} and C^{α}–N bonds on the two sides of the methylene linker, which is different to the cleavage of the amide bond itself seen in most amide cases. Theoretical calculations and isotopic labeling experiments demonstrate that the phenyl ring regulates the proton transfer reactions. The proton directly migrates to the C^{β} position *via* a 1,5-H shift leading to the efficient loss of benzene, while it stepwise migrates to the amide nitrogen resulting in the formation of a benzyl cation. The stepwise proton transfer is achieved *via* intramolecular proton-transport catalysis. The C^{γ} position accepts the proton from the carbonyl oxygen *via* a 1,6-H shift, and then donates it to the amide nitrogen *via* a 1,4-H shift. The general 1,3-H shift from the carbonyl oxygen to the amide nitrogen can be excluded in this case due to its significant energy barrier. The substituent effects are also applied to explore the reaction mechanism, and it proves that both C^{β} and C^{γ} are involved in the dissociative proton transfer processes. For monosubstituted *N*-benzylbutyrolactams, the abundance ratios of the two competing product ions are well correlated with the nature of the substituents.

Introduction

Protonation and proton transfer (PT) are of fundamental importance in numerous chemical and biochemical reactions.[1,2] The interpretation of a reaction mechanism usually begins with the determination of the site(s) of protonation and the subsequent proton transfers. Mass spectrometry has become an important tool in the fundamental studies of protonation and proton transfers of molecules in the gas phase. On the other hand, a clear understanding of the occurrence of protonation and proton transfers is quite desirable for structure elucidation when using electrospray ionization (ESI) mass spectrometry. The positive charge brought in by protonation is usually the driving force for fragmentation reactions of the protonated molecules ($[M + H]^+$), *i.e.*, so-called dissociative proton attachement.[3–5]

Department of Chemistry, Zhejiang University, Hangzhou, 310027, China. E-mail: panyuanjiang@zju.edu.cn, suncuirong@zju.edu.cn; Fax: +86 571 87951629; Tel: +86 571 87951264

† Electronic supplementary information (ESI) available: Additional calculations discussed in the text, CID mass spectra, NMR spectra of key compounds, and figures, cartesian coordinates, total energies, zero point energy corrections and the number of imaginary frequencies of all optimized structures discussed in the text at the B3LYP/6-31++G(d,p) level. See DOI: 10.1039/c1ob06020a

However, it is often observed that no fragmentation takes place when a molecule is protonated at the thermodynamically favored site. In contrast, the fragmentations occur when the proton migrates to some specific sites which are less favorable for protonation, though. Such specific positions were recently described as dissociative protonation sites, which are reactive centers in ESI mass spectrometry.[6,7] Fragmentations initiated by dissociative proton transfer,[8–11] from the basic center to the reactive center (Scheme 1), are sometimes hindered by an energy barrier or spatial distance. The proton transfers can be promoted through solvent assistance or neighbouring group participation.[12–15] The

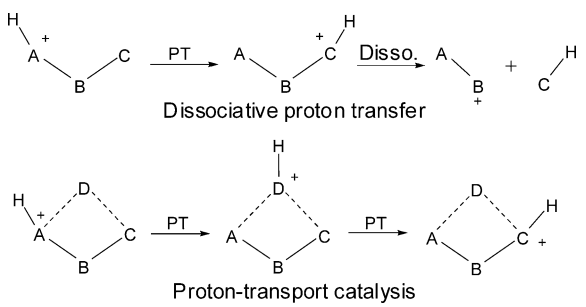

Scheme 1

energy barrier for the proton transfer can be reduced as a result of interaction with an external molecule or an internal group. Such catalytic effect is known as proton-transport catalysis (Scheme 1).[16–22]

The reactions of amides have been extensively studied because of the significance of this group in chemistry, biochemistry and chemical biology; moreover, the amide linkage is the basic constituent of peptides and proteins. Due to the development of soft ionization techniques such as ESI and MALDI, mass spectrometry has become an increasingly popular tool for the study of proteins. The collision-induced dissociation (CID) mass spectra of protonated peptides provide abundant sequence information such as the most typical N-terminal, b_n, and C-terminal, y_n, series of sequence ions,[23] which arise from the cleavage of amide bonds. The correct interpretation of the CID spectra of protonated peptides is an arduous task because they are usually very complicated. During the CID fragmentations of peptides, intramolecular hydrogen transfers frequently take place before the dissociation,[24–29] which increase the difficulties of spectra interpretation. In the past two decades, the "mobile proton model"[30–36] has been widely applied in dealing with the fragmentation of protonated peptides and proteins in mass spectrometry. Based on this model, before fragmentation, the extra proton migrates from a higher gas-phase basicity but unreactive site, to an energetically less favored but reactive site.

The decomposition of amides is naturally used as a model reaction in studying the cleavage of peptide bonds of proteins. Amide bond cleavage is one of the most typical and important reactions for amide compounds both in solution and in the gas phase.[35,37–39] Due to the tremendous amount of effort by several researchers over the past few decades, it has been agreed that in most cases, the most basic site of an amide is the carbonyl oxygen.[40,41] However, there is a clear distinction between amide bond cleavage in solution and that found in the gas phase. The acid-catalyzed amide hydrolysis in aqueous solution may be subdivided in four reaction steps, including O-protonation, water attacking the carbonyl carbon, N-protonation, and C–N bond breaking.[37,38] In contrast, the major fragmentation of protonated simple amides observed in the gas phase is the disruption of the amide bond, leading to loss of amine or ammonia, which is triggered by protonation at the amide nitrogen (charge-driven). As isolation from solvent molecules, a 1,3-proton transfer prior to the fragmentations, from the carbonyl oxygen to the amide nitrogen, is necessary, though the energy of the N-protonated species is higher than that of the O-protonated species, and the energy barrier between the two isomers is considerably higher. In the case of formamide,[41] the differences in energies of the two isomers is 60 kJ mol^{-1} and the energy barrier for the conversion between the two isomers is 289 kJ mol^{-1}. In some β-lactam drugs, penicillin G as a typical example,[42,43] the dominant fragmentation of its $[M + H]^+$ ion is the cleavage of the β-lactam bond, which requires the lactam nitrogen to be protonated. In the fragmentation of protonated *N*-benzylbutyrolactams in mass spectrometry, we observed that the major fragmentations are the cleavages of C^{α}–C^{β} and C^{α}–N bonds instead of the cleavage of the amide bond. We report here the results of a combined experimental and theoretical investigation on intramolecular proton transfers during the CID process for protonated *N*-benzylbutyrolactams, which play central roles in the characteristic fragmentation reactions.

Experimental

Mass spectrometry

All CID experiments were performed using a Bruker Esquire 3000^{plus} mass spectrometer (Bruker-Franzen Analytik GmbH, Bremen, Germany) equipped with an ESI source and an ion trap analyzer in the positive-ion mode. Nitrogen was used as the nebulizing gas at a pressure of 10 psi and the drying gas at a flow rate of 5 L min^{-1}. The drying gas temperature was set at 250 °C and the capillary voltage was set at –4000 V. Solutions were infused to the mass spectrometer with a syringe pump at a flow rate of 6 μL min^{-1}. The CID mass spectra were obtained with helium as the collision gas at an appropriate collision energy after isolation of the desired precursor ion. In the substituent effects study, the fragmentation amplitude was fixed at a voltage of 0.60 V.

Accurate masses were measured on an Apex III (7.0 Tesla) Fourier transform ion cyclotron resonance (FTICR) mass spectrometer (Bruker, Billerica, MA, USA) equipped with an ESI source in the positive-ion mode. Sodium trifluoroacetate was used as an external calibration compound. Nitrogen was used as the nebulizing gas and the drying gas. Argon was used as the collision gas. The capillary voltage was set at –4269 V, and the drying gas temperature was set at 150 °C.

Theoretical calculations

All theoretical calculations were carried out using the Gaussian 03 package of programs.[44] Candidate structures of the reactants, products, intermediates and transition states were first optimized at the B3LYP/6-31G(d) level of theory, and then further optimized at the B3LYP level of theory with the 6-31++G(d,p) basis set. No symmetry constraints were imposed on the optimizations. The reaction pathways were traced forward and backward by the intrinsic reaction coordinate (IRC) method. All optimized structures were subjected to vibrational frequency analysis to ensure a transition state having only one imaginary vibrational frequency while a local or global minimum having no imaginary vibrational frequency. Vibrational frequencies and zero-point energies (ZPE) for all the key species were calculated at the same level of theory. The energies discussed here are the sum of electronic and thermal energies.

Sample synthesis and preparation

The *N*-benzylbutyrolactams were synthesized and purified according to previous reported procedures[45] using the corresponding benzyl bromides and butyrolactam. 4-hydroxybenzyl chloride was used instead for the synthesis of *N*-(4-hydroxybenzyl)butyrolactam. The structures were confirmed by ^1H and ^{13}C NMR spectroscopy and mass spectrometry. *N*-benzylbutyrolactam (**5**), ^1H NMR ($CDCl_3$, 500 MHz): δ 7.16–7.29 (m, 5H), 4.38 (s, 2H), 3.20 (t, 2H), 2.42 (t, 2H), 1.92 (m, 2H); ^{13}C NMR ($CDCl_3$, 125 MHz): δ 175.7, 136.4, 128.9, 128.3, 127.8, 47.0, 46.9, 31.1, 17.8; HRMS calc for $C_{11}H_{14}NO^+$ ([**5** + H]$^+$): 176.1070, found: 176.1064.

Samples were dissolved in methanol first, and then diluted with methanol–water (1 : 1, v/v) containing 0.5% formic acid. Methanol-d_4 containing 0.1% trifluoroacetic acid-d_1 was used as solvent for the deuterium labeling experiment to form an $[M + D]^+$ ion.

Table 1 Relative abundances of product ions in the CID spectra of protonated *N*-benzylbutyrolactams (fragmentation amplitude 0.60V)[a]

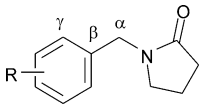

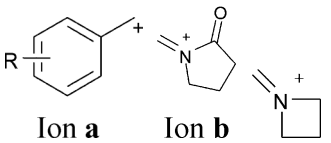

Compound	*R*	[M + H]$^+$	Ion **a**	Ion **b**	
1	*p*-OH	192 (0.2)[b]	107 (8.5)	98 (100)	70 (2.3)
2	*p*-OC_2H_5	220 (1.4)	135 (100)	98 (66.1)	70 (1.7)
3	*p*-OCH_3	206 (0.5)	121 (44.2)	98 (100)	70 (2.9)
4	*p*-CH_3	190 (2.4)	105 (8.0)	98 (100)	70 (3.5)
5	H	176 (7.7)	91 (18.4)	98 (100)	70 (4.2)
6	*p*-^{35}Cl	210 (30.3)	125 (18.0)	98 (100)	70 (5.7)
7	*p*-^{79}Br	254 (31.2)	169 (31.5)	98 (100)	70 (1.0)
8	*p*-CF_3	244 (100)	159 (36.4)	98 (22.3)	70 (1.9)
9	*p*-NO_2	221 (100)	136 (2.7)	98 (6.5)	70 (0.8)
10	*m*-OH	192 (16.5)	107 (100)	98 (34.3)	70 (2.1)
11	*m*-OCH_3	206 (13.1)	121 (100)	98 (20.7)	70 (1.5)
12	*m*-NO_2	221 (100)	136 (5.4)	98 (7.6)	70 (0.8)
13	*m*-CH_3	190 (11.0)	105 (23.5)	98 (100)	70 (4.7)
14	*m*-^{35}Cl	210 (100)	125 (32.8)	98 (65.2)	70 (5.5)

[a] For other ions for some compounds, see the CID spectra in the ESI†. [b] *m*/*z* (Relative abundance %).

Results and discussion

Fragmentation of protonated *N*-benzylbutyrolactams

In the CID experiments of all protonated *N*-benzylbutyrolactams studied (Table 1), two major fragmentation reactions, C^{α}–C^{β} and C^{α}–N bond cleavage, leading to a loss of benzene (or substituted benzene) and butyrolactam, respectively, were observed. The nomenclature for C^{α}, C^{β} and C^{γ} is shown in Table 1. In all these cases, amide bond cleavage for the [M + H]$^+$ ions was not observed. The minor product ion at *m*/*z* 70 was attributed to the secondary fragmentation of the product ion at *m*/*z* 98, as confirmed by the MS^3 experiment. Compound **5** is employed as a model compound to study the reaction mechanism. The CID mass spectrum of protonated compound **5** is shown in Fig. 1. The ion derived from a loss of butyrolactam (*m*/*z* 91) probably has a benzyl structure. Previous theoretical studies have revealed that the conversion of the benzyl cation to a tropylium ion involves a significant energy barrier (about 280 kJ mol^{-1}).[46,47] In ESI mass spectrometry, fragmentation of benzylated cations prefers to generate benzyl cations,[48–55] notwithstanding a few exceptions which have been reported in which the tropylium ion can be co-produced in the fragmentation of benzylpyridiniums.[56–58]

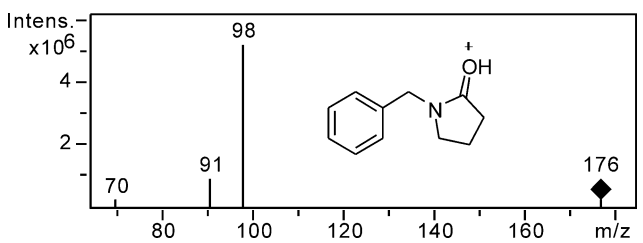

Fig. 1 CID mass spectrum of the [M + H]$^+$ ion of *N*-benzylbutyrolactam (compound **5**).

Dissociative proton transfer

The *N*-benzylbutyrolactams may be protonated at different positions, including the carbonyl oxygen, the amide nitrogen, the phenyl ring and the polar substituent. However, the fragmentations take place only when the proton is attached upon the dissociative positions, the amide nitrogen or C^{β} of the phenyl ring, as shown in Scheme 2. Taking compound **5** as an example, the relative energies of species protonated at different positions are shown in Scheme 2, which were calculated at the B3LYP/6-31++G(d,p) theoretical level. The most favorable protonation site is the carbonyl oxygen that is similar to other simple amides. The computed relative energy for protonation at C^{β} is 99.6 kJ mol^{-1} higher than that at the carbonyl oxygen and 44.1 kJ mol^{-1} higher than that at the amide nitrogen. Interestingly, ion **b** (*m*/*z* 98) is still the predominant product ion in the fragmentation of protonated compound **5**, even more preponderant than ion **a** (*m*/*z* 91). Moreover, theoretical calculations for compounds **3** and **9** (Table S1, ESI†) indicate that the carbonyl oxygen-protonated species is still the most stable. In this respect, the proton transfers may control the fragmentation reactions rather than the proton affinities (PAs)[59] of the dissociative positions. From the initial stable protonated species to the final reactive protonated species, the conversion should be achieved through the most energetically favorable route among all possible proton transfer pathways.

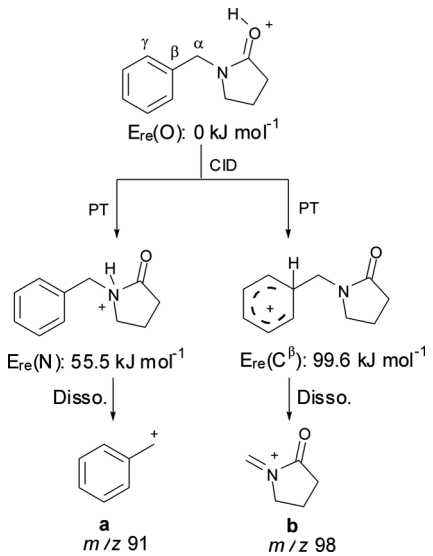

Scheme 2 Proposed fragmentation mechanism of protonated *N*-benzylbutyrolactam.

Intramolecular proton-transport catalysis

The migration of the ionizing proton was studied by theoretical calculations. A schematic potential energy diagram for the two fragmentation reactions of protonated *N*-benzylbutyrolactam is given in Fig. 2. Full details of the structures and energies of species involved are presented in the ESI†.

The formation of ion **a** requires the amide nitrogen to be protonated. The N-protonation is usually one of the necessary

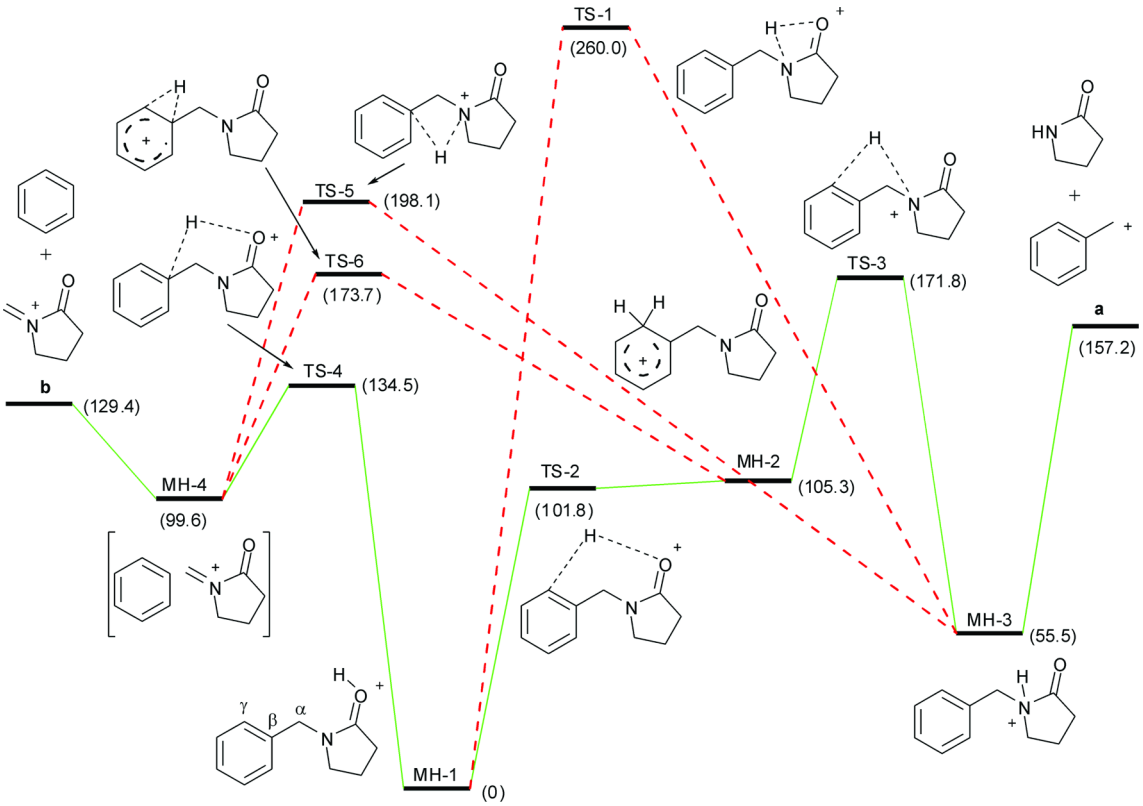

Fig. 2 Potential energy diagram for the fragmentation of protonated *N*-benzylbutyrolactam using DFT calculations at the B3LYP/6-31++G(d,p) level. Relative energies are given in kJ mol^{-1}.

steps for the amide bond cleavages both in solution[37–39,60] and in the gas phase.[61,62] Interconversion of the N-protonated species and the O-protonated species of amides in the gas phase is generally accepted as a 1,3-H shift.[41] For *N*-benzylbutyrolactam, the activation energy for 1,3-H shift (TS-**1**) is 260.0 kJ mol^{-1}. Besides this direct proton transfer route, the calculations suggest another energetically more favored indirect pathway, in which the proton first migrates to the C$^{\gamma}$ of the phenyl ring *via* a 1,6-H shift (TS-**2**) and then to the nitrogen *via* a 1,4-H shift (TS-**3**). The total activation energy of this stepwise transfer is significantly lower (88.2 kJ mol^{-1}) than that of the direct 1,3-H shift. Although the PA of C$^{\gamma}$ position is lower than that of the oxygen and the nitrogen, the phenyl ring acts as an intramolecular catalyst that can accept a proton from the oxygen and release it at the nitrogen through lowering the proton transfer barrier. As a consequence, formation of the N-protonated species is unlikely to be achieved through a 1,3-H shift. The C$^{\gamma}$-participated two-step proton transfer is more reasonable in terms of energy. It is noteworthy that when zero-point vibrational energies and thermal corrections are included, the relative energy of TS-**2** is lower than that of MH-**2**. Cases such as this are not unusual.[63,64]

Since theoretical calculations indicated that the phenyl ring (C$^{\gamma}$ position) promoted proton migration from the carbonyl oxygen to the amide nitrogen, deuterium labeling experiments were performed to verify this prediction. The CID mass spectrum of the [M + D]$^+$ ion of *N*-benzylbutyrolactam is shown in Fig. 3a. The product ions at *m*/*z* 91 and *m*/*z* 92 are both attributable to benzyl cations. When the deuteron firstly migrates to the phenyl ring, it may subsequently migrate to the nitrogen or be retained

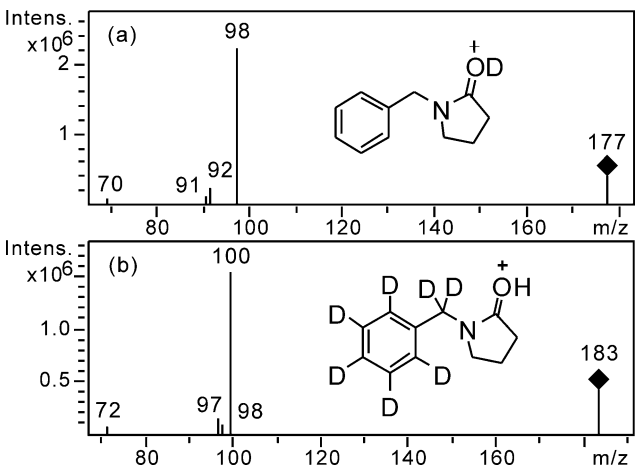

Fig. 3 CID mass spectra of the (a) [M + D]$^+$ ion of *N*-benzylbutyrolactam (*m*/*z* 177) and (b) [M + H]$^+$ ion of *N*-(benzyl-d$_7$)butyrolactam (*m*/*z* 183).

on the phenyl ring (a proton migrates to the nitrogen instead) in the subsequent transfer, which leads to the generation of product ions $C_7H_7^+$ (*m*/*z* 91) and $C_7H_6D^+$ (*m*/*z* 92) simultaneously. Coincidentally, in the CID mass spectrum of the [M + H]$^+$ ion of *N*-(benzyl-d$_7$)butyrolactam (Fig. 3b), two signals that are attributable to benzyl cations appear, that is, $C_7HD_6^+$ (*m*/*z* 97) and $C_7D_7^+$ (*m*/*z* 98). These isotopic ions were confirmed by their accurate masses determined on a FTICR mass spectrometer (Table 2). It provides convincing evidence that the phenyl ring is involved in generation of product ion **a**. It is noteworthy that the H/D exchange may

Table 2 Accurate masses of product ions in the fragmentation of the $[M + D]^+$ ion of compound **5** and the $[M + H]^+$ ion of compound **5**-d_7

Compound	Measured mass	Calculated mass	Error (ppm)	Elemental composition
5	177.1131	177.1133	−1.1	$C_{11}H_{13}DNO^+$
	98.0601	98.0600	−1.0	$C_5H_8NO^+$
	92.0605	92.0605	0	$C_7H_6D^+$
	91.0542	91.0542	0	$C_7H_7^+$
5-d_7	183.1509	183.1509	0	$C_{11}H_7D_7NO^+$
	100.0726	100.0726	0	$C_5H_6D_2NO^+$
	98.0982	98.0982	0	$C_7D_7^+$
	97.0919	97.0919	0	$C_7HD_6^+$

not be limited to the *ortho* positions of the phenyl ring. Further H/D exchanges along the whole phenyl ring are also possible because the proton ring-walk is well known for arenium ions formed in the gas-phase.[65–67] The *meta* or *para* position-involved 1,2-H shifts do not affect the fragmentation reactions, so they were not focused on and further explored in this study. In addition, the benzylic methylene group is not involved in H/D exchange that is confirmed by the fragmentation of the $[M + H]^+$ ion of $C_6H_5CD_2$–$NCO(CH_2)_3$ (Figure S17, ESI†).

Once the proton arrives at C^β of the phenyl ring, the C^α–C^β bond is broken spontaneously (observed in calculation) to form an ion/neutral complex (MH-**4**). Loss of a benzene from MH-**4** yields ion **b**. Three proton transfer pathways should be considered (Fig. 2), but two of these are not energetically favourable. Proton migration from nitrogen to the C^β position (TS-**5**) is inhibited due to its high activation energy (198.1 kJ mol^{-1}). In another route, a 1,2-H shift from the C^γ to C^β (TS-**6**, 173.7 kJ mol^{-1}) of the phenyl ring is also unfavorable. The energy barrier for direct proton transfer from the carbonyl oxygen to the C^β position (TS-**4**) is only 134.5 kJ mol^{-1} because on chemical grounds, a 1,5-H shift *via* a six-membered transition state is energetically favorable. This 1,5-H shift is also sterically favored. For the optimized geometry of MH-**1** (Scheme S1, ESI†), the proton is located on the carbonyl oxygen, but it also interacts with the phenyl ring. Therefore, proton transfers from the oxygen to the C^β or C^γ position are relatively easy.

In these two fragmentation reactions, the rate controlling step is the 1,4-H shift (TS-**3**) for the formation of ion **a** and the 1,5-H shift (TS-**4**) for the formation of ion **b**, respectively. TS-**4** is 37.3 kJ mol^{-1} lower in energy than TS-**3**. On the other hand, the total energy of ion **b** and benzene is 27.8 kJ mol^{-1} lower than that of ion **a** and butyrolactam. Consequently, the generation of ion **b** is more favorable than that of ion **a** in terms of energy and this is consistent with the experimental results.

Substituent effects

Substituent effects are very useful in exploring reaction mechanisms.[68,69] In order to better understand the reaction mechanism, a series of compounds with different substitutes at *para* or *meta* positions of the phenyl ring were investigated. All these compounds undergo similar fragmentation reactions (Table 1), though a few substituents (*p*-CF_3 and *p*-NO_2) themselves can be eliminated (these additional reactions are independent and not discussed here). The variation in abundance of the two alternative product ions, $C_5H_8ON^+$ and $RC_6H_4CH_2^+$ (where R is a substituent) which are formed in competition, correlates well with the nature of the substituents. As shown in Fig. 4, the $\ln[(C_5H_8ON^+)/(RC_6H_4CH_2^+)]$ values are in line with σ_{pm}. σ_{pm} is a linear combination of the Hammett substituent constants,[70] σ_p^+ and σ_m, obtained by fitting the experimental data that is illustrated below. In fact, the correlation of $\ln[(C_5H_8ON^+)/(RC_6H_4CH_2^+)]$ *versus* σ_p^+ (or σ_m) alone is random and irregular.

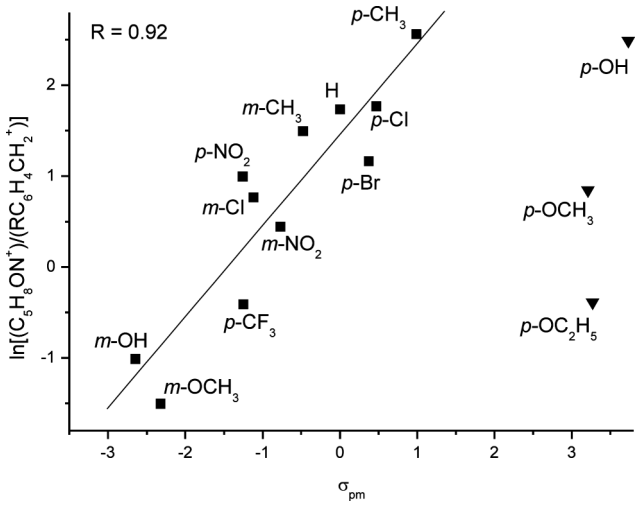

Fig. 4 Plot of $\ln[(C_5H_8ON^+)/(RC_6H_4CH_2^+)]$ *versus* the σ_{pm} values for the CID reactions of the $[M + H]^+$ ions of *N*-benzylbutyrolactams monosubstituted at the *para* or *meta* position.

In view of the nitrogen and C^β of the phenyl ring competing for the ionizing proton through different proton transfer pathways, with a substituent on the phenyl ring, the sensitivities of TS-**3** and TS-**4** to structural changes are different because the electronic effect of a substituent on C^β and C^γ is different (see substituent constants in Table 3). As shown in Scheme 3, a *para* substituent exhibits a *para* effect on TS-**4** and a *meta* effect on TS-**3**, while a *meta* substituent exhibits a *meta* effect on TS-**4** and a *para* effect on TS-**3**. It indicates that the *para* and *meta* substituent effects (σ_p^+ and σ_m) must be considered together.[68] The intensity ratios of the peaks corresponding to these two ions reflect the competition between the two alternative fragmentation pathways. Both the

Table 3 Hammett substituent constants and logarithmic values of the intensity ratios for the two product ions, **a** and **b**[a]

Compound	σ_p^+	σ_m[b]	σ_{pm}	ln **b**/**a**
1	−0.92	0.12	3.73	2.488
2	−0.81	0.10	3.27	−0.389
3	−0.78	0.12	3.21	0.845
4	−0.31	−0.07	0.99	2.560
5	0	0	0	1.734
6	0.11	0.37	0.47	1.770
7	0.15	0.39	0.37	1.165
8	0.61	0.43	−1.25	−0.408
9	0.79	0.71	−1.26	0.995
10	−0.92	0.12	−2.65	−1.011
11	−0.78	0.12	−2.32	−1.505
12	0.79	0.71	−0.77	0.442
13	−0.31	−0.07	−0.48	1.494
14	0.11	0.37	−1.12	0.768

[a] σ_p^+ and σ_m values from ref. 70 [b] σ_m values was used as no σ_m^+ values could be obtained.

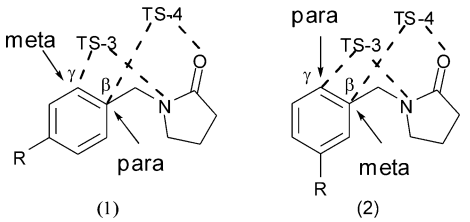

Scheme 3 The electronic effects of a substituent on the two reaction-controlling proton transfers.

para and *meta* substituent effects of a substituent influence the intensity ratio (**b** over **a**). With the variation in substituents, the $\ln[(C_5H_8ON^+)/(RC_6H_4CH_2^+)]$ values should follow eqn (1) for *para*-monosubstituted *N*-benzylbutyrolactams and eqn (2) for *meta*-monosubstituted *N*-benzylbutyrolactams. Exhilaratingly, a variety of monosubstituted compounds tested here agree with these two equations very well. By applying the multiple regression method (data in Table 3), we got $k_p = -3.745$, $k_m = 2.395$, $R^2 = 0.84$. Thus, for *para* substituents, $\sigma_{pm} = -3.745\ \sigma_p^+ + 2.395\ \sigma_m$, and for *meta* substituents, $\sigma_{pm} = -3.745\ \sigma_m + 2.395\ \sigma_p^+$.

$$\ln [(C_5H_8ON^+)/(RC_6H_4CH_2^+)] = k_p \cdot \sigma_p^+ + k_m \cdot \sigma_m + t = \sigma_{pm} + t \quad (1)$$

$$\ln [(C_5H_8ON^+)/(RC_6H_4CH_2^+)] = k_p \cdot \sigma_m + k_m \cdot \sigma_p^+ + t = \sigma_{pm} + t \quad (2)$$

By studying the substituent effects on the distribution of the product ions, the reaction mechanism has been further proven. Accordingly, the reaction is mainly governed by the activation energy of proton transfers. Taking *m*-OH and *m*-OCH_3 substituted compounds (compounds **10** and **11**) as typical examples, these two substituents considerably reduce the energy barriers towards proton transfer between O and C^γ (TS-**2**), and between C^γ and N (TS-**3**), due to their strong electron-donating effect on C^γ (σ_p^+ = –0.92 and –0.78, respectively), but they slightly raise the energy barrier towards proton transfer between O and C^β (TS-**4**) due to their electron-withdrawing effect on C^β ($\sigma_m = 0.12$). The theoretical calculations also support such substituent effects (Figure S18, ESI†). The activation energies of TS-**2** and TS-**3** for the *m*-OH substituted compound are 39.2 kJ mol^{-1} and 27.4 kJ mol^{-1} lower than that for the unsubstituted compound, respectively; while the activation energy of TS-**4** for the *m*-OH substituted compound is 0.6 kJ mol^{-1} higher than that for the unsubstituted compound. As a result, *m*-$HOC_6H_4CH_2^+$ and *m*-$CH_3OC_6H_4CH_2^+$ are the dominant product ions in their corresponding mass spectra. Furthermore, the stability of the products is not the key factor for fragmentation reactions. For example, compared with the unsubstituted compound, *p*-CH_3 ($\sigma_p^+ = -0.31$) slightly stabilizes the benzyl cation but the formation of *p*-$CH_3C_6H_4CH_2^+$ is less favored. Similarly, *p*-CF_3 ($\sigma_p^+ = 0.61$) sharply destabilizes the benzyl cation but the formation of *p*-$CF_3C_6H_4CH_2^+$ is more favored. Such insight that the relative stability of the fragment ions is not the decisive factor has also been known for the fragmentation of arenium ions.[71–73] However, the *para*-strong electron-donating group (*p*-OH, *p*-OCH_3 and *p*-OC_2H_5) substituted compounds are exceptions which deviate from the general linear correlation. The formation of ion **b** (loss of substituted benzene) in the fragmentation of these compounds is not as efficient as expected. Because the benzyl cation can be highly stabilized by the *para*-strong electron-donating groups,[7] the stability of the product ions becomes another important factor influencing the reaction in these special cases.

Conclusions

In the fragmentation of protonated *N*-benzylbutyrolactams, losses of benzene (or substituted benzene) and butyrolactam were observed as the major reactions rather than the cleavage of the amide bond. Based on the combination of theoretical calculations and experimental studies, it was found that the ionizing proton is floating between several positions and the activation energy of proton transfer steps controls the fragmentations. When the dissociative protonation sites (amide N and C^β) capture the external proton, fragmentation reactions can take place. From the thermodynamically stable but unreactive site (carbonyl O) to the dissociative sites, the external proton migrates directly to C^β and stepwise to N. The phenyl ring acts as an intramolecular catalyst promoting proton transfer from the carbonyl O to amide N. The present work extends and enriches our knowledge on mobile features of the ionization proton and fragmentation patterns of amide compounds.

Acknowledgements

The authors gratefully acknowledge financial support from the National Science Foundation of China (Nos. 21025207 and 20975092).

Notes and references

1 S. Scheiner, *Acc. Chem. Res.*, 1985, **18**, 174.
2 K. S. Peters, *Acc. Chem. Res.*, 2009, **42**, 89.
3 E. Uggerud, *Mass Spectrom. Rev.*, 1992, **11**, 389.
4 J.-L. M. Abboud, R. Notario, E. Ballesteros, M. Herreros, O. Mó, M. Yáñez, J. Elguero, G. Boyer and R. Claramunt, *J. Am. Chem. Soc.*, 1994, **116**, 2486.
5 O. Mó, M. Yáñez, J.-F. Gal, P. C. Maria and J.-C. Guillemin, *J. Phys. Org. Chem.*, 2002, **15**, 509.
6 Y.-P. Tu, *J. Org. Chem.*, 2006, **71**, 5482.
7 N. Hu, Y.-P. Tu, Y. Liu, K. Jiang and Y. Pan, *J. Org. Chem.*, 2008, **73**, 3369.
8 G. I. Mackay, A. C. Hopkinson and D. K. Bohme, *J. Am. Chem. Soc.*, 1978, **100**, 7460.
9 L. González, O. Mó and M. Yáñez, *J. Phys. Chem. A*, 1998, **102**, 1356.
10 A. Meffert and J. Grotemeyer, *Int. J. Mass Spectrom.*, 2001, **210/211**, 521.
11 D. B. Milligan, P. F. Wilson, C. G. Freeman, M. Meot-Ner and M. J. McEwan, *J. Phys. Chem. A*, 2002, **106**, 9745.
12 A. J. Kresge, *Acc. Chem. Res.*, 1975, **8**, 354.
13 C. A. Bayse, *Org. Biomol. Chem.*, 2011, **9**, 4748.
14 B. S. Souza, S. F. Yunes, M. F. Lima, J. C. Gesser, M. M. Sá, H. D. Fiedler and F. Nome, *Org. Biomol. Chem.*, 2011, **9**, 6163.
15 A. Furmanchuk, O. Isayev, L. Gorb, O. V. Shishkin, D. M. Hovorun and J. Leszczynski, *Phys. Chem. Chem. Phys.*, 2011, **13**, 4311.
16 D. K. Bohme, *Int. J. Mass Spectrom. Ion Processes*, 1992, **115**, 95.
17 A. J. Chalk and L. Radom, *J. Am. Chem. Soc.*, 1997, **119**, 7573.
18 J. W. Gauld and L. Radom, *J. Am. Chem. Soc.*, 1997, **119**, 9831.
19 P. J. A. Ruttink, P. C. Burgers, L. M. Fell and J. K. Terlouw, *J. Phys. Chem. A*, 1998, **102**, 2976.
20 M. A. Trikoupis, J. K. Terlouw and P. C. Burgers, *J. Am. Chem. Soc.*, 1998, **120**, 12131.
21 D. Schröder, J. Roithová, P. Gruene, H. Schwarz, H. Mayr and K. Koszinowski, *J. Phys. Chem. A*, 2007, **111**, 8925.
22 M. George, V. S. Sebastian, P. N. Reddy, R. Srinivas, D. Giblin and M. L. Gross, *J. Am. Soc. Mass Spectrom.*, 2009, **20**, 805.
23 K. Biemann and I. A. Papayannopoulos, *Acc. Chem. Res.*, 1994, **27**, 370.

24 A. G. Harrison and T. Yalcin, *Int. J. Mass Spectrom. Ion Processes*, 1997, **165/166**, 339.
25 J. Buijs, C. Hagman, K. Håkansson, J. H. Richter, P. Håkansson and S. Oscarsson, *J. Am. Soc. Mass Spectrom.*, 2001, **12**, 410.
26 F. Tureček and E. A. Syrstad, *J. Am. Chem. Soc.*, 2003, **125**, 3353.
27 T. J. D. Jørgensen, H. Gårdsvoll, M. Ploug and P. Roepstorff, *J. Am. Chem. Soc.*, 2005, **127**, 2785.
28 S. Molesworth, C. M. Leavitt, G. S. Groenewold, J. Oomens, J. D. Steill and M. van Stipdonk, *J. Am. Soc. Mass Spectrom.*, 2009, **20**, 1841.
29 D. R. Mueller, M. Eckersley and W. J. Richter, *Org. Mass Spectrom.*, 1988, **23**, 217.
30 A. R. Dongré, J. L. Jones, Á. Somogyi and V. H. Wysocki, *J. Am. Chem. Soc.*, 1996, **118**, 8365.
31 V. H. Wysocki, G. Tsaprailis, L. L. Smith and L. A. Breci, *J. Mass Spectrom.*, 2000, **35**, 1399.
32 B. Paizs and S. Suhai, *Mass Spectrom. Rev.*, 2005, **24**, 508.
33 C. A. Morrison, M. M. Siddick, P. J. Camp and C. C. Wilson, *J. Am. Chem. Soc.*, 2005, **127**, 4042.
34 N. C. Polfer, J. Oomens, S. Suhai and B. Paizs, *J. Am. Chem. Soc.*, 2007, **129**, 5887.
35 B. J. Bythell, S. Suhai, Á. Somogyi and B. Paizs, *J. Am. Chem. Soc.*, 2009, **131**, 14057.
36 R. Boyd and Á. Somogyi, *J. Am. Soc. Mass Spectrom.*, 2010, **21**, 1275.
37 R. S. Brown, A. J. Bennet and H. Slebocka-Tilk, *Acc. Chem. Res.*, 1992, **25**, 481.
38 D. Zahn, *J. Phys. Chem. B*, 2003, **107**, 12303.
39 W. Y. Tsang, N. Ahmed and M. I. Page, *Org. Biomol. Chem.*, 2007, **5**, 485.
40 C. L. Perrin, *Acc. Chem. Res.*, 1989, **22**, 268.
41 H.-Y. Lin, D. P. Ridge, E. Uggerud and T. Vulpius, *J. Am. Chem. Soc.*, 1994, **116**, 2996.
42 E. Daeseleire, H. De Ruyck and R. Van Renterghem, *Rapid Commun. Mass Spectrom.*, 2000, **14**, 1404.
43 C. K. Fagerquist, A. R. Lightfield and S. J. Lehotay, *Anal. Chem.*, 2005, **77**, 1473.
44 M. J. Frisch, G. W. Trucks, H. B. Schlegel, G. E. Scuseria, M. A. Robb, J. R. Cheeseman, J. A. Montgomery Jr., T. Vreven, K. N. Kudin, J. C. Burant, J. M. Millam, S. S. Iyengar, J. Tomasi, V. Barone, B. Mennucci, M. Cossi, G. Scalmani, N. Rega, G. A. Petersson, H. Nakatsuji, M. Hada, M. Ehara, K. Toyota, R. Fukuda, J. Hasegawa, M. Ishida, T. Nakajima, Y. Honda, O. Kitao, H. Nakai, M. Klene, X. Li, J. E. Knox, H. P. Hratchian, J. B. Cross, C. Adamo, J. Jaramillo, R. Gomperts, R. E. Stratmann, O. Yazyev, A. J. Austin, R. Cammi, C. Pomelli, J. W. Ochterski, P. Y. Ayala, K. Morokuma, G. A. Voth, P. Salvador, J. J. Dannenberg, V. G. Zakrzewski, S. Dapprich, A. D. Daniels, M. C. Strain, O. Farkas, D. K. Malick, A. D. Rabuck, K. Raghavachari, J. B. Foresman , J. V. Ortiz, Q. Cui, A. G. Baboul, S. Clifford, J. Cioslowski, B. B. Stefanov, G. Liu, A. Liashenko, P. Piskorz, I. Komaromi, R. L. Martin, D. J. Fox, T. Keith, M. A. Al-Laham, C. Y. Peng, A. Nanayakkara, M. Challacombe, P. M. W. Gill, B. Johnson, W. Chen, M. W. Wong, C. Gonzalez and J. A. Pople. *Gaussian 03, Revision B*, Gaussian, Inc., Pittsburgh, PA, 2003.
45 J. Mun and M. B. Smith, *Synth. Commun.*, 2007, **37**, 813.
46 T. D. Fridgen, J. Troe, A. A. Viggiano, A. J. Midey, S. Williams and T. B. McMahon, *J. Phys. Chem. A*, 2004, **108**, 5600.
47 C.-H. Shin and S.-J. Kim, *J. Korean Chem. Soc.*, 2005, **49**, 247.
48 M. Edelson-Averbukh and A. Mandelbaum, *J. Mass Spectrom.*, 2003, **38**, 1169.
49 J. Bialecki, J. Ruzicka and A. B. Attygalle, *J. Mass Spectrom.*, 2006, **41**, 1195.
50 E.-L. Zins, C. Pepe and D. Schröder, *J. Mass Spectrom.*, 2010, **45**, 1253.
51 K. V. Barylyuk, K. Chingin, R. M. Balabin and R. Zenobi, *J. Am. Soc. Mass Spectrom.*, 2010, **21**, 172.
52 Y. Chai, K. Jiang and Y. Pan, *J. Mass Spectrom.*, 2010, **45**, 496.
53 D. Kuck, H.-F. Grützmacher, D. Barth, S. Heitkamp and M. C. Letzel, *Int. J. Mass Spectrom.*, 2011, **306**, 159.
54 Y. Chai, H. Sun, Y. Pan and C. Sun, *J. Am. Soc. Mass Spectrom.*, 2011, **22**, 1526.
55 Y. Chai, K. Jiang, C. Sun and Y. Pan, *Chem.–Eur. J.*, 2011, **17**, 10820.
56 E.-L. Zins, C. Pepe, D. Rondeau, S. Rochut, N. Galland and J.-C. Tabet, *J. Mass Spectrom.*, 2009, **44**, 12.
57 E.-L. Zins, D. Rondeau, P. Karoyan, C. Fosse, S. Rochut and C. Pepe, *J. Mass Spectrom.*, 2009, **44**, 1668.
58 E.-L. Zins, C. Pepe and D. Schröder, *Faraday Discuss.*, 2010, **145**, 157.
59 E. P. L. Hunter and S. G. Lias, *J. Phys. Chem. Ref. Data*, 1998, **27**, 413.
60 A. Williams, *J. Am. Chem. Soc.*, 1976, **98**, 5645.
61 Y.-P. Tu and A. G. Harrison, *J. Am. Soc. Mass Spectrom.*, 1998, **9**, 454.
62 B. Paizs, M. Schnölzer, U. Warnken, S. Suhai and A. G. Harrison, *Phys. Chem. Chem. Phys.*, 2004, **6**, 2691.
63 C. F. Rodriquez, A. Cunje, T. Shoeib, I. K. Chu, A. C. Hopkinson and K. W. Michael Siu, *J. Am. Chem. Soc.*, 2001, **123**, 3006.
64 H. E. Aribi, C. F. Rodriquez, D. R. P. Almeida, Y. Ling, W. W.-N. Mak, A. C. Hopkinson and K. W. Michael Siu, *J. Am. Chem. Soc.*, 2003, **125**, 9229.
65 D. Kuck, *Mass Spectrom. Rev.*, 1990, **9**, 583.
66 D. Kuck, *Int. J. Mass Spectrom.*, 2002, **213**, 101.
67 D. Kuck, In *The Encyclopedia of Mass Spectrometry*, vol. 4, N. M. M. Nibbering (Ed.), Elsevier, Amsterdam, 2005, 229–242/270–286.
68 H. Tanida, *Acc. Chem. Res.*, 1968, **1**, 239.
69 T. M. Krygowski and B. T. Stępień, *Chem. Rev.*, 2005, **105**, 3482.
70 C. Hansch, A. Leo and R. W. Taft, *Chem. Rev.*, 1991, **91**, 165.
71 D. Kuck and H.-F. Grützmacher, *Org. Mass Spectrom.*, 1978, **13**, 81.
72 D. Kuck and H.-F. Grützmacher, *Org. Mass Spectrom.*, 1978, **13**, 90.
73 D. Kuck, *Mass Spectrom. Rev.*, 1990, **9**, 187.